Available online at www.sciencedirect.com

ScienceDirect

Energy Procedia 43 (2013) 86 – 92

Energy Procedia

4th Workshop on Metallization for Crystalline Silicon Solar Cells

The multi-busbar design: an overview

Stefan Braun[a], Giso Hahn[a], Robin Nissler[b], Christoph Pönisch[b], Dirk Habermann[b]*

[a] University of Konstanz, Department of Physics, 78457 Konstanz, Germany
[b]Gebr. Schmid GmbH, Robert-Bosch-Str.32-36, Freudenstadt 72250, Germany

Abstract

The demand for highly efficient photovoltaic modules at low costs leads to new solar cell designs. For enhanced module efficiency the cell efficiency has to be optimized regarding later operation under module conditions. This implies that the interconnected solar cell structure has to be assessed. Commonly the solar cell itself is optimized separately.
In this work an easy to implement cell design was investigated where the number of busbars was varied to decrease the total series resistance of the interconnected solar cell. For this study a simulation program based on the two-diode model was applied to determine the optimal efficiency of the device. Furthermore, the simulations revealed that a device with multiple busbars has a high potential in cost savings due to a reduction in metal consumption for the front side metallization. For an optimized cell structure the amount of Ag paste needed for a sufficient front side metallization could be reduced to 7 mg Ag paste for a 6 inch solar cell. In the same time the efficiency can be increased. A detailed simulation of a screen printed and stringed rear side of a multi-busbar solar cell revealed the amount of rear side pads necessary for a sufficient interconnection leading to low series resistances.

Selection and peer-review under responsibility of Guy Beaucarne, Gunnar Schubert and Jaap Hoornstra

Keywords: Multi-Busbar Design; Ag Cost Reduction; Interconnected Solar Cells

1. Introduction

Future solar cell designs not only have to take into account an increase of efficiency but also reduced production costs to be competitive on the growing solar market. A big cost factor is the screen printed Ag front side metallization. Today solar cells are assessed on cell level but it is beneficial to take a closer look to the solar cell performance under module conditions. In the recent past attempts have been

* Stefan Braun. Tel.: +49-7531-88-2082; fax: +49-7531-88-3895.
E-mail address: Stefan.Braun@uni-konstanz.de

Selection and peer-review under responsibility of Guy Beaucarne, Gunnar Schubert and Jaap Hoornstra
doi:10.1016/j.egypro.2013.11.092

undertaken to optimize the 3-busbar cell design by adding more busbars to the device [1]. In this paper an approach is discussed where the number and geometry of the busbars is varied leading to a significant reduction of Ag paste consumption and in the same time boosting the module efficiency.

2. Simulation

To simulate the IV characteristics of a solar cell the two-diode model [2] is used. Equation (1) with voltage U, current density j, photo-generated current density j_{ph}, series resistance R_s, shunt resistance R_p, temperature T, Boltzmann constant k_B, saturation current densities of the two diodes j_{01} and j_{02} and ideality factors n_1 and n_2 has to be solved iteratively:

$$j(U) = -j_{ph} + j_{01} * \left(e^{\frac{U-j(U)*R_S}{n_1*k_B*T}} - 1 \right) + j_{02} * \left(e^{\frac{U-j(U)*R_S}{n_2*k_B*T}} - 1 \right) + \frac{U-j(U)*R_S}{R_p} \quad (1)$$

As a reference, we assumed a state of the art industrial solar cell with an efficiency of 19.2% [3]. This can e.g. be achieved by using selective emitter technology and a properly optimized screen printing technique with full area Al-BSF (Back Surface Field). The 90 µm wide fingers have a low line resistance of 0.22 Ω/cm, the specific contact resistance is 1.5 mΩcm^2. For the simulation we set the parameters necessary for equation (1) as n_1= 1, n_2= 2, j_{01}= 538 fA/cm^2, j_{02}= 17 nA/cm^2, R_p= 10000 Ωcm^2, j_{ph}= 40.5 mA/cm^2 at a temperature of 25°C, representing a p-type monocrystalline 6 inch Czochralski wafer of 200 µm thickness with a resistivity of 2 Ωcm, alkaline textured, plasma-enhanced chemical vapor deposition SiN_x coating and a 80/50 Ω/sq selectively etched back emitter. The finger spacing was set to 2.1 mm. The assumed busbar width is 1.5 mm. For the contribution of the series resistance one has to add all components of a solar cell as described in [4].

To simulate the series resistance of the Al back contact we solved a partial differential equation (PDE) of Poisson form assuming a continuous Ag/Al pad of 1.5 mm width on the rear side and an Al layer with a sheet resistance of 6.3 mΩ/sq. This was done by 3D simulation using the program FlexPDE 6 [5]. The width of the Al/Ag pads at the rear side for the wire design was assumed to be similar to the wire diameters. Line and contact resistance for the screen printed metal fingers were determined by four point probe measurements of comparable solar cells [6]. Also a continuous solder contact for the busbars/fingers and Al/Ag was assumed. The two-diode model describes a homogeneous solar cell without finger interruptions or variations in sheet resistivity. Additionally, a change of R_s under illumination has to be taken into account. Especially for cells with high R_s this is not negligible [7,8].

Two different measurement setups were simulated. For the measurement of the IV-curve the solar cell is placed on a metallized chuck to collect the current contacting the complete rear contact. For the front contact multiple pins are collecting the current from the busbars. In the simulation a setup with 12 pins for each busbar was simulated. Each busbar has a width of 1.4 mm. This setup can be seen in Fig. 1, left side.

In the second scenario a stringed front side was simulated. This simulation corresponds to the picture shown in Fig 1 right side. On each busbar a collector ribbon with a height of 200 µm and the width of the busbars was simulated. The contact resistance between the Cu ribbon and the busbar was set to 0 Ω because it is negligible for a continuously soldered contact area. The current is then collected on the edge of the solar cell on one side only.

A comparison of different ribbon geometries was performed using optical calculations to give a rough estimation of the effectively shaded area of such ribbons. A widely used rectangular Sn coated Cu ribbon was compared with a round Sn coated Cu wire on cell and on module level. In the calculation it was assumed that the refraction index of the glass and the EVA foil are identical. For the calculation the absorption of the Sn, glass and EVA layer was neglected.

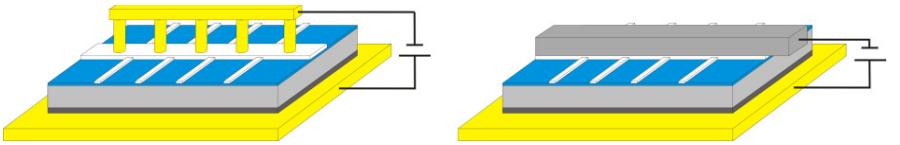

Fig. 1. IV measurement of solar cells: (left) The current pins on the busbar underestimate the series resistance of the front side metallization. (right) A stringed solar cell where the current is collected on the edge of the cell is a more representative measurement for a device which will be integrated in a module

Another beneficial effect of the multi-busbar design is the reduction of the effective finger length (half the finger length between two busbars or wires) which can be used to reduce the amount of metal used for the front side metallization. A simulation was performed taking into account the optimal finger spacing and width using an aspect ratio for the finger metallization of 0.5. If the simulation was carried out on cell level, the optimal efficiency was calculated and the amount of metal needed was determined.

The sheet resistance of the screen printed Al layer was set to 10 mΩ/sq., corresponding to an Al layer thickness of 18 µm. The pad geometry on the rear was set to 4 mm x 0.5 mm and the assumption was made that the current can only flow over the contact pads into the Cu wires. The current is collected on one edge of the solar cell only by the wires. In the simulation the number of rear pads and the wire thickness was varied for a multi-busbar cell with 15 round Cu wires. In addition one continuous pad with the dimension of 152 mm x 0.5 mm was simulated. The thickness variation of the Cu wires was between 220 µm and 300 µm.

3. Results of the simulation

The results of the first simulation are displayed in Fig 2. By adding flat busbars to the device the efficiency decreases because of additional shading of the 1.4 mm wide busbars (black line). The decreased series resistance cannot increase the efficiency because the current is directly collected on the busbars via multiple probes (compare with Fig. 1 left side).

This changes when the current is collect via tabbings on the front side (dashed red line). For a cell with four busbars the efficiency slightly rises because the drop in series resistance dominates over the additional shading. Going to five busbars the shading dominates the structure again and the efficiency decreases.

For an optimized busbar width one can observe a different behavior. In the green line one can observe the efficiency increase by adding more busbars to the cell structure. This phenomenon can be explained by a reduction of busbar width with increasing number of busbars. It is displayed in Fig 2 by the blue dashed line.

The comparison of a rectangular ribbon with a round wire demonstrated the beneficial form of the wire because of a significant reduction in shading. In Fig. 3 both geometries are shown under module conditions.

One aspect that was not taken into account for the simulation is the effective shading of the wires. The effective shading of the wires has to be calculated by ray tracing simulation. For a detailed analysis the absorption, roughness and the material of the wire should be taken into account, too, but first approximations show very promising results. The effective shading of a wire is much lower in case of perpendicular incidence beams will be reflected on the wire and will to a certain extent hit the wafer surface, whereas nearly all beams descending on a rectangular busbar tabbing with rounded edges will not get in contact with the wafer surface. Both cases can be seen in Fig. 3.

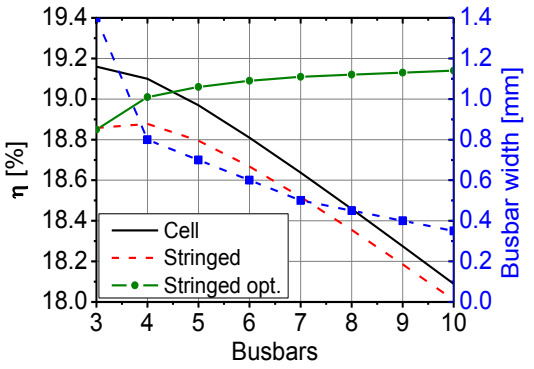

Fig. 2. Simulated cell efficiency plotted over the number of busbars. The black line shows the device contacted with multiple pins on busbars. The dashed red line shows the device with a stringed front side (using tabbings contacted at the cell's edge). The thicker green line shows an adapted busbar design where the width is optimized for each amount of flat busbars. The blue dashed line displays the optimal busbar width.

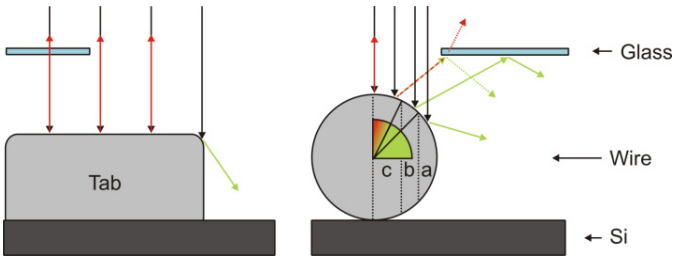

Fig. 3. Rays descending on a busbar tabbing (left) and on a round wire (right). The wire can be divided into three regions. Black arrows indicate the descending rays, green rays will reach the surface of the cell and red rays will not reach the surface.

For a round wire there are three regions of importance. In region (a) the beam is directly reflected onto the surface of the cell. Therefore, the effectively shaded area is reduced to 70.1% of the actual area. In region (b) the reflected rays from the wire are totally reflected at the module glass. Assuming a refraction index of 1.5 for the module glass the effectively shaded area is reduced to 35.7%. In region (c) the reflected rays from the round wire are reflected again on the module glass, but now the incident angle is larger than the angle of total reflection, therefore the beam is divided into a reflected and a transmitted part. This will also decrease the effectively shaded area of the wire and leads to higher short-circuit currents [9].

Using 15 wires instead of three busbars the finger length can be reduced to 5 mm instead of 25 mm for a front design with three busbars. This offers the possibility to reduce the amount of metal needed for the front side metallization. In Fig. 4 one can observe a rapid rise of the area weighted series resistance of the front grid of a 3-busbar solar cell with decreasing finger width. In contrast, for the wire solar cell the resistance rises only slowly. This is directly related to the reduced finger length of such a device with 15 wires. Using advanced printing technologies it would be possible to reduce the finger width significantly and in the same time obtain a low series resistance contribution of the finger grid.

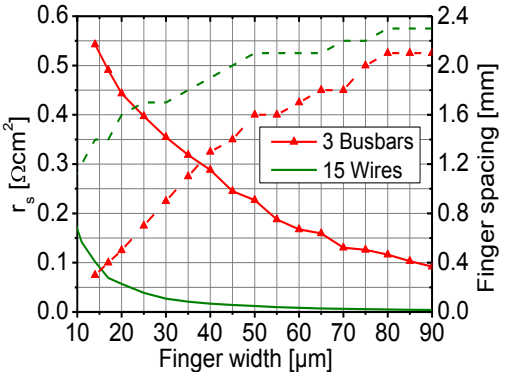

Fig. 4. Finger width of a 3-busbar and a multi-busbar solar cell with 15 round Cu wires. On the left y-axis the area weighted series resistance contribution of the finger grid is plotted and shown in solid lines. On the right y-axis the optimized finger spacing is plotted and shown in the dashed lines.

For the optimized finger spacing shown in the dashed lines in Fig 4 a decrease with decreasing finger width is visible. The drop is higher for the 3-busbar solar cell.

The optimization of the efficiency leads to the optimal Ag paste consumption for the front side metallization. In Fig. 5 left side the efficiencies for both cell designs are correlated to the finger widths. The maximum efficiency reachable for the 3-busbar design is in the range of 19.3%. The finger width is in the range of 50 µm because a finger length of 25 mm needs a sufficient line conductivity. For the multi-busbar solar cell the finger width can be reduced to 17 µm and still the series resistance contributions stays low. The optimal efficiency lies in the range of 19.7% for the multi-busbar solar cell.

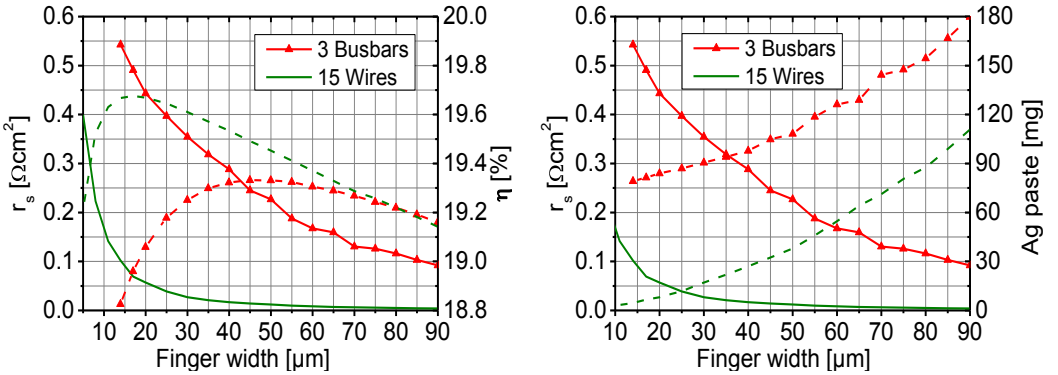

Fig. 5. On the left side the finger width is plotted over the optimized efficiency for both cell designs (dashed lines). On the right side the silver consumption can be seen in the dashed lines.

Going to the right side of Fig. 5 the amount of Ag paste is plotted instead of the efficiency (dashed lines). Both dashed lines indicate that a reduction of finger width leads to a reduced metal consumption. Taking a look at the optimal efficiencies the Ag consumption for the 3-busbar solar cell is 108 mg where the multi-busbar solar cell design only needs 6.8 mg Ag paste. With this result a screen printed front grid with 17 µm wide fingers with an aspect ratio of 0.5 and a finger spacing of 1.5 mm leads to efficiencies in the range of 19.7%.

For the rear side optimization of a stringed multi-busbar solar cell a wide window of parameters was found. Increasing the number of rear pads for a given wire diameter leads to a series resistance reduction. In the same time a larger wire diameter offers the possibility to decrease the number of rear pads. These results are plotted in Fig. 6.

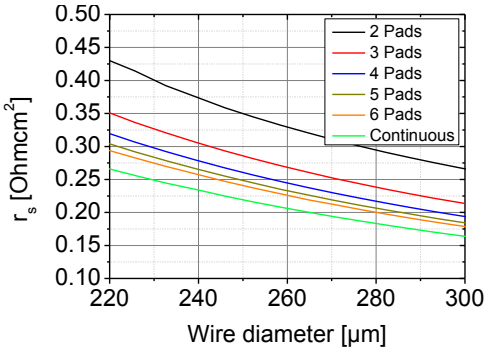

Fig. 6. Series resistance contribution of an Al screen printed rear side stringed with 15 Cu wires.

Allowing a maximal series resistance of <0.3 Ωcm^2 various combinations are possible to obtain a low series resistance contribution of the stringed rear side. Using Ag pads for the rear side contact one should keep in mind that an increased number of pads leads to a reduction of the open circuit voltage because of an increased recombination at the pad surface if the Ag pads are in direct contact with the Si.

First experimental results on cell and module level show similar efficiencies on cell level for the 3-busbar and multi-busbar technology in the area of 19.4%. But on module level the multi-busbar technology shows 0.3-0.4%$_{abs}$ higher efficiencies up to 18.6%, mainly due to a lower series resistance leading to higher fill factors [10].

4. Conclusion

Using two-diode model simulations it was demonstrated that an increased number of busbars leads to higher module efficiencies because of a reduced series resistance of the stringed device. Optimizing the width of the busbars leads to an additional rise in efficiency. The reduction of the effective finger length has additional beneficial effects for the solar cell device. Using 15 busbars instead of three, the finger width can be significantly reduced, offering the possibility of massive metal reduction on the front side. The optimized finger width for a multi-busbar solar cell lies in the range of 17 µm with an Ag consumption of only 6.8 mg for a 6 inch solar cell. The optimized 3-busbar structure consumes 108 mg of Ag paste.

An analysis of the stringed Al printed rear side revealed a broad window of parameters. Combining thick wire diameters of 300 µm with only two pads on the rear side still leads to a sufficiently low series resistance contribution of the rear side.

Acknowledgements

The authors would like to thank Lisa Mahlstädt for assistance during processing and the company Gebr. Schmid GmbH for the funding of this project.

References

[1] Schneider A, Rubin L, Rubin G. Solar cell improvement by new metallization techniques - The DAY4™ electrode concept. Proc. 4th WC PEC, Waikoloa 2006, p. 1095-8
[2] Chan DSH, Phang JCH. Analytical methods for the extraction of solar-cell single- and double-diode model parameters from I-V characteristics. IEEE Trans Electron Dev 1987;34:286-93.
[3] Tjahjono B, Haverkamp H, Wu V, Anditsch HT, Jung WH, Cheng J, et al. Optimizing selective emitter technology in one year of full scale production. Proc. 26th EU PVSEC, Hamburg 2011, p. 901-5
[4] Mette A. New concepts for front side metallization of industrial silicon solar cells. Dissertation University of Freiburg; 2007.
[5] FlexPDE, PDE Solutions, http://www.pdesolutions.com
[6] Schroder DK. Semiconductor materials and device characterization. 3rd ed. Hoboken, New Jersey: Wiley; 1979.
[7] Aberle AG. Wenham SR, Green MA. A new method for accurate measurement of the lumped series resistance of solar cells. Proc. 23th IEEE PVSC, Louisville 1993, p. 133-9
[8] Fong K, McIntosh K, Blakers AW. Accurate series resistance measurement of solar cells. Progr Photovolt Res Appl 2011;DOI: 10.1002/pip.1216
[9] Blakers AW. Shading losses of solar-cell metal grids. J Appl Phys 1992;7:5237-41.
[10] Braun S, Hahn G, Nissler R, Pönisch C, Habermann D. Multi-busbar solar cells and modules: higher efficiencies and low silver consumptions. Energy Procedia 2013; in press.